Experimental Investigations of the Ignition and Flame Stabilization of a Full Cone Kerosene Spray in a Lab-scale Model Combustor

G.C. Gebel*, T. Mosbach, W. Meier, M. Aigner
Institute of Combustion Technology, German Aerospace Center (DLR)
70569 Stuttgart, Germany

Abstract

This paper presents experimental investigations of the ignition of a kerosene spray in a lab-scale model combustor with well-defined boundary conditions. The experiments were intended to capture the transient ignition process, starting with a flame kernel and completing with a stable flame. Ignition was achieved by laser-induced breakdowns. High-speed Particle Image Velocimetry was applied to the spray to measure the average velocity vectors of the fuel droplets and to verify its suitability as a tool for spray characterization. An ignition probability study was carried out to determine the ignition probability of the spray flame with respect to the location of the laser-induced breakdown. Simultaneous Planar Laser-Induced Fluorescence measurements on fuel aromatics and hydroxyl radicals (OH) were performed to obtain detailed information about the fuel density distribution and location of the chemical reaction zone during the ignition and flame stabilization. The results are valuable data for model development and validation.

Introduction

Spark ignition of liquid fuel sprays in air and the subsequent flame kernel growth are complex processes, subjected to a variety of mechanisms. A deep understanding is essential for the development of theoretical and numerical models, which contribute to improved efficiency and emission of gas turbines or piston engines. The specific background of this study is the aero-engine relight at high altitude. The ability of such engines to ignite under harsh ambient conditions, as they exist at high flight levels, is a key requirement of the certification process [1]. Furthermore, modern aero-engine combustors commonly use lean combustion systems, which enforce the challenge of altitude relight. The development of such combustors requests the ability to perform numerical simulation of the ignition process, since an iterative development including extensive testing, cannot be performed in an economic manner. The ignition of a gas turbine combustor is divided into three phases [2]:

- Phase 1: Formation of a self-sustainable flame kernel of sufficient size and temperature. Gas turbines typically have spark plugs to form the initial flame kernels.
- Phase 2: Subsequent growth and propagation of the flame from the kernel location to the entire combustion zone. This process depends on fuel evaporation rates, the flow field inside the combustor and combustion kinetics.
- Phase 3: Flame spread from one combustor section to the nearby ones. Aviation gas turbines are equipped with up to twenty combustor sections, which do not necessarily possess individual spark plug devices.

This paper attends to phenomena occurring during phase 2. The laser-induced ignition of a kerosene spray was investigated in a lab-scale model combustor with well-defined boundary conditions. The experiments were intended to capture the transient ignition process, starting with a flame kernel and completing with a stable flame. The obtained data were utilized to verify numerical simulations of spray ignition processes at DLR with the codes THETA and SPRAYSIM [3,4]. The model combustor was a vertically arranged flow channel, which provided good optical access to enable the application of optical measurement techniques. The fuel was either Jet A-1 aviation kerosene or Exxsol D80, a kerosene-like solvent. In a first step the droplet velocity distribution of the spray was investigated. High-speed Particle Image Velocimetry (HS-PIV) was applied to the spray. The usage of PIV for spray characterization was applied in only few studies [5,6,7]. The standard techniques for spray velocity measurements are Laser Doppler Anemometry (LDA) or its extension Phase Doppler Anemometry (PDA). However, only HS-PIV visualizes the instantaneous velocity fields and therefore allows the investigation of spray dynamics with high spatial and temporal resolution. In this paper we give average results from this experiment. Furthermore, an ignition probability study was performed to find the most reliable location for the laser-induced breakdowns which were used as ignition sparks. Finally, the flame kernel growth and flame stabilization were investigated with Planar Laser-induced Fluorescence (PLIF) on OH radicals and fuel aromatics.

* Corresponding author: gregor.gebel@dlr.de

Experimental Methods

Model combustor and ignition laser

The combustor was a vertically arranged flow channel with a nearly square cross-section of 62 cm^2 and a length of one meter. Three sides were equipped with windows to provide extensive access for optical measurement techniques. The back of the channel was mounted to a translation stage which allowed horizontal and vertical shifting. A schematic of the model combustor is shown in Figure 1. The fuel injector was a commercial full cone spray nozzle from Delavan/Goodrich, type SN 30609-2. It provided a weakly swirling full-cone spray with a cone angle of approximately 40 degrees and a droplet diameter range from 20 to 50 µm. The nozzle was supplied with fuel and atomizat air via two vertical pipes. The fuel reservoir was a bottle with a double hull design. The inner hull represented a siphon bottle which contained the fuel. It was set under an overpressure of Δp = 100 mbar through pressurized air from an in-house air supply system. The overpressure resulted in a fuel mass flow of approximately 20 g/min. It was manually set by an air valve and monitored through a potentiometric pressure sensor. The chamber between the outer and the inner hull was part of a water circuit system. Water circulated between the chamber and a Lauda C 6 laboratory thermostat. This system allowed adjustment of the fuel temperature, which was set to 294 K and measured by a thermocouple inside the reservoir. The temperature was selected close to ambient temperature and therefore could be sustained with very high accuracy. A continuous air co-flow streamed through the flow channel from top to bottom at atmospheric pressure. The co-flow inlet was a sintered steel ring on top of the flow channel. The air co-flow and the atomization air were controlled via two Bronkhorst mass flow controllers. In this paper air flows are given according to the units used by the two mass flow controllers: Air co-flows are given in m^3/h and atomization air flows are given in standard litres per minute (slm). The co-flow temperature was measured to be 288 K by thermocouples inside the flow channel. It resulted from expansion from a 6-bar in-house air supply system. A frequency-doubled Nd:YAG laser type InnoLas Spitlight 600 created the laser-induced breakdowns to ignite the spray. Breakdowns were of the non-resonant type, which is initiated by multiphoton ionization and followed by electron cascade breakdown. Physically, this mechanism reveals a high degree of similarity with spark discharge [8]. The laser provided 6-ns-pulses of approximately 300 mJ at 532 nm in a single pulse mode. Breakdowns were achieved by expanding the laser beams to a diameter of approximately 40 mm and refocusing them via a laser-grade achromatic doublet lens with a focal length of 120 mm. The laser beams entered the flow channel with a downward angle of 30 degrees. The usage of laser-induced ignition offered some significant advantages over spark discharge ignition: First, no hardware which may disturb the experimental boundary conditions had to be mounted inside the flow channel. Second, the Spitlight 600 laser offered accurate triggering with an uncertainty of only 10 ns. Third, the breakdown location can be varied freely. Finally, the reproducibility of the features (location, transient size and shape, energy content) of a laser-induced breakdown is superior compared to a spark discharge. Flame quenching was achieved by a nitrogen injection system, which automatically engaged after a laser pulse. Fuel vapour and burnt gases were aspirated by a ventilator-driven exhaust system at the bottom of the flow channel. Unburnt liquid fuel was captured by a funnel and collected in a can at the very bottom.

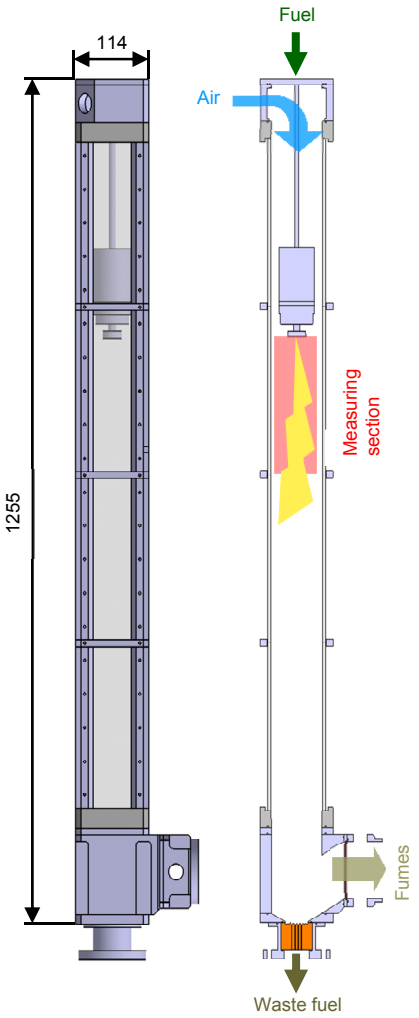

Figure 1 Schematic of the model combustor. Scales are given in mm.

Spray velocity measurements

HS-PIV measurements were performed on the kerosene spray for various air and fuel mass flows to obtain spatially resolved velocity information. The laser sheet was created by a dual-head Nd:YAG slab laser type EdgeWave Innoslab IS6II-DE. It was operated in a double pulse mode at a repetition rate of 5 kHz for each laser head. The pulse separation time between both heads was set to 15 µs. The laser beam was expanded by appropriate optics to a vertical sheet with a height of 58 mm and a thickness of about 1 mm. The laser sheet entered the flow channel through the same window as the ignition laser beam and radially penetrated the spray directly be-

low the injector. A high-speed camera type LaVision HighSpeedStar 6 was mounted in front of the flow channel and oriented perpendicularly to the laser sheet plane. The camera was equipped with a Tokina 100 mm f/2.8 macro lens. The aperture was set to f/16. A stack of broadband transmission filters with an overall transmission of 5 % was mounted in front of the lens. The camera was set into a double frame mode with a recording frequency of 5 kHz, an exposure time of 1 µs and a resolution of 768 × 768 pixels. The field-of-view was estimated to be 22 × 19 mm with a calibration target type LaVision 7. The laser and the camera were triggered by separate trigger pulses from a BNC-DDPG565 pulse generator. During one measurement 1000 double-frames were recorded, to gain sufficient data for averaging. Figure 2a gives a schematic of the HS-PIV setup.

Ignition probability tests

An ignition probability survey on the kerosene spray was carried out to find the most reliable sparking location in dependence of the air co-flow and atomization air flow. The pulse energy of the ignition laser was not the focus of this survey and was kept at a constant level. The radial location of the breakdown was kept at a constant position of 4 mm from the spray centre axis. Ignition probability tests were performed for breakdown positions of 1, 2, 3 and 4 cm downstream of the nozzle. The air co-flow and atomization air flow were varied for each position.

Planar Laser-induced Fluorescence measurements

PLIF measurements were performed to obtain information about the fuel density distribution and flame front location. A tunable UV laser system was used to induce fluorescence of OH molecules in the chemical reaction zone and of fuel aromatics. Figure 2b gives a schematic of the PLIF setup.

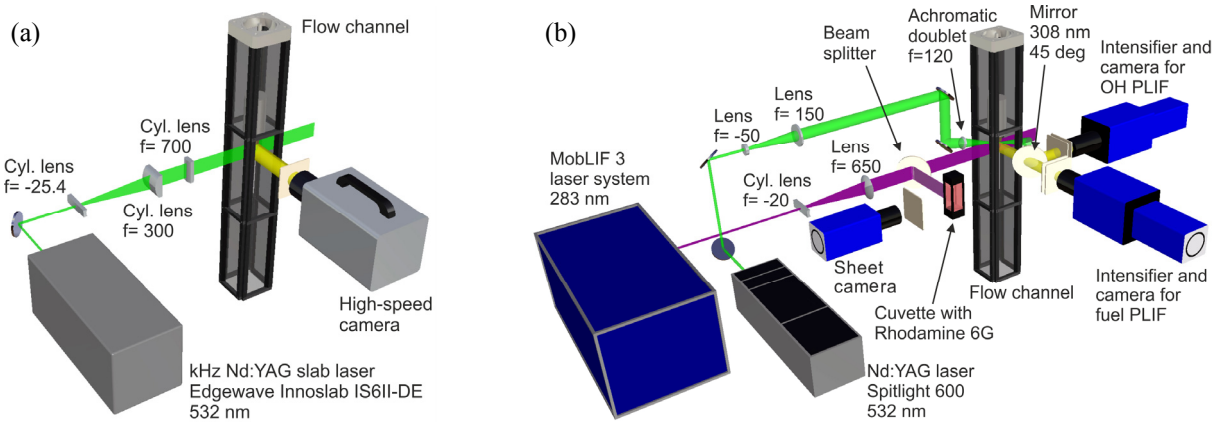

Figure 2 (a) Setup of the HS-PIV experiment, (b) setup of the PLIF experiment.

The PLIF laser system consisted of a dual-head Nd:YAG pumping laser type Spectra Physics PIV-400-10 and a frequency-doubled tunable dye laser type Sirah PRSC-G-24-EG. Both were mounted in an air-conditioned container (MobLIF 3 in Fig. 2b) for protection and temperature stabilization. The laser system was operated at a sustained repetition rate of 10 Hz. The dye was Rhodamine 6G; the dye laser was tuned to $\lambda = 282.75$ nm, corresponding to the $Q_1(5)$ transition of OH within the vibrational band $v = 1 \leftarrow 0$ of the $A^2\Sigma^+$-$X^2\Pi$ system. The laser pulses had an energy of 6 mJ and a pulse length of 7 ns. The spectral position of the excitation line was verified in advance of the measurements with the laminar methane-air flame of a matrix burner. The laser beam was expanded by appropriate optics to a vertical sheet with a height of 92 mm and a thickness of about 0.5 mm. A fraction of the laser sheet was deflected by a beam splitter into a quartz cuvette filled with a fluorescent dye solution (Rhodamine 6G in ethanol). The fluorescence profile within the cuvette was imaged by a CCD camera type LaVision Imager Intense 3 with a Nikon 50 mm f/1.4 lens parallel to the fluorescence measurements. The profile was used for correcting laser sheet inhomogeneities. The fluorescence signals from the OH and the fuel aromatics were simultaneously imaged by two intensified camera systems, each consisting of a CCD camera type LaVision Imager Intense 3 and a LaVision I/I IRO 25 image intensifier. Both cameras were equipped with UV-transparent Nikon 105 mm f/4.5 macro lenses. The first camera system captured the fuel fluorescence and was placed in front of the flow-channel with a direct view to the ignition region. Two Schott WG295 filters in front of the lens blocked scatter light and reflections from the UV laser beam. The second camera system was mounted perpendicularly to the first one and viewed the ignition region via a dichroic mirror, which had a highly reflecting coating for the UV regime from 290 to 317 nm. The mirror separated the OH signal from the overall fluorescence and directed it towards the second camera system. The remaining fluorescence signal passed through the mirror towards the first camera system. Two interference filters (range 295 to 304 nm) were placed in front of the second camera system to improve the purity of the recorded OH fluorescence signal. All devices

of the measurement system were triggered by a BNC-DDPG565 pulse generator. The image intensifiers were set to an exposure time of 200 ns. The cameras were operated at a resolution of 1049 × 1393 pixels. The field-of-view was estimated to be 68.5 × 90.9 mm with a calibration target type LaVision 7. The delay between the ignition laser pulse and the measurement system was varied, in order to capture different moments of the ignition process. For each delay the measurements were repeated several times for a statistical analysis. Twenty ignitions were performed for every delay. Every camera recorded one image for each ignition.

Results and Discussion

Spray velocity measurements

HS-PIV measurements of the spray were performed for air co-flows of 20, 40, 60 and 80 m^3/h, atomization air flows of 6.5, 12.5 and 18.5 slm and a reservoir Δp of 100 mbar. The fuel was Jet A-1 kerosene. The post-processing of the images was performed with the FlowMaster module of the software DaVis 7.2. The cross correlation algorithm for the vector calculation had to be adjusted very carefully because of the wide range of droplet velocities: The two images of each double-frame were cross-correlated in three loops. The final interrogation windows had a resolution of 32 × 32 pixels. With respect to the wide velocity range, an interrogation window shift of 20 ± 20 m/s in vertical direction was applied to the first correlation loop. The primary breakup zone, which spreads 5 mm downstream of the nozzle, was masked out. Fuel densities were too high to accomplish a cross-correlation in this regime. Average vector fields were calculated from the 1000 double-frames per measurement, representing the spray from 0.7 to 19.2 mm downstream of the nozzle with a resolution of 48 × 43 vectors. Only vectors which appear on at least 25 % of the instantaneous vector fields were taken into account for the average vector field. This procedure suppressed the statistical effects of single droplets which were separated from the spray cone. The usage of the high-speed technique did not only allow average spray velocity measurements, but also gave insights into fluctuations. The latter results are not presented in this paper. Figure 3 shows exemplary vector fields for co-flows of 20 and 80 m^3/h and atomization air mass flows of 6.5, 12.5 and 18.5 slm. The background colors represent absolute droplet velocities. The spray features a narrow core region with average droplet velocities extending from 15 to 30 m/s. With increasing distance from the centre axis, velocities decrease to approximately 5 m/s and then re-increase to velocities of 8 to 10 m/s near the spray cone edges. A comparison of the average vector fields for different parameters indicates a significant impact of the atomization air flow on the spray, while changes of the air co-flow only have a minor effect. Streamlines in the core region show a drift to the right. It results from the alignment tolerance of the laser sheet, which corresponded to the sheet thickness of 1 mm. Therefore, the laser sheet radially penetrated the spray with a horizontal accuracy of approximately ±1 mm. Radial velocities are the highest in the core region and therefore become visible. However, since the effect is small, basic findings of the experiment are not affected.

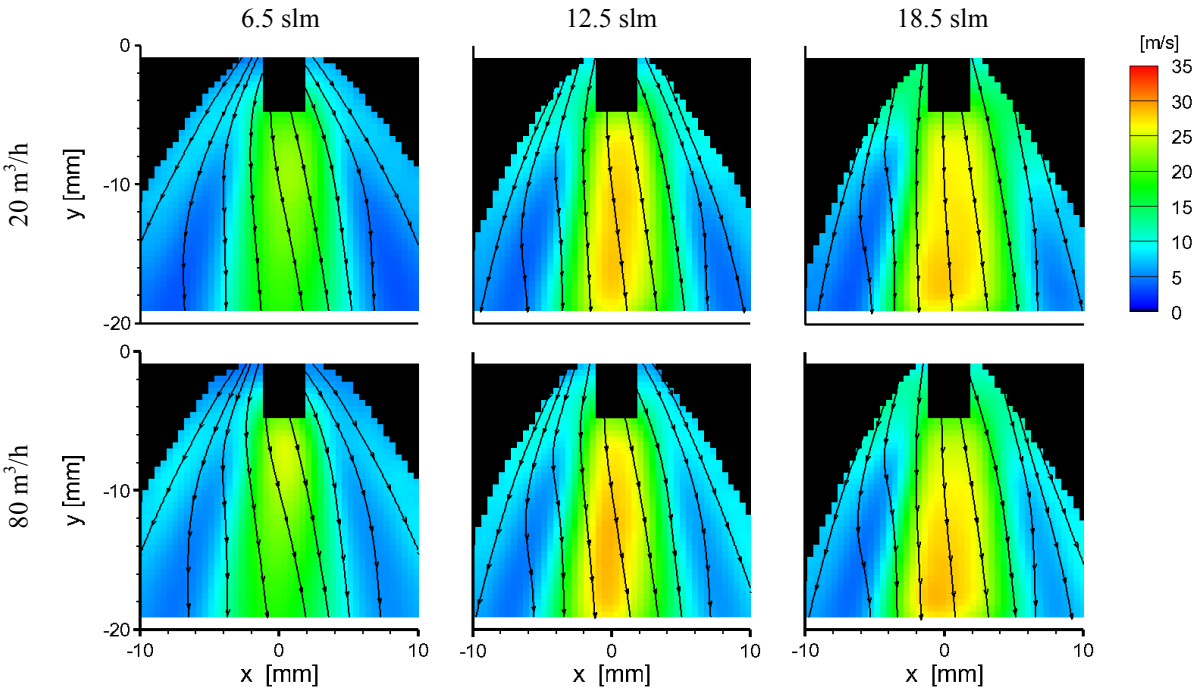

Figure 3 Exemplary results from the HS-PIV measurements, average velocity fields.

Figure 4 shows two graphs with velocity spectra which were obtained from the average vector fields. The occurrence of a velocity represents its fraction on all detected velocities, with a range from 0 to 100 %. Both histograms feature the same basic appearance: they range from minimum 2 m/s to maximum 30 m/s and show a higher peak at very low velocities and a smaller peak at very high velocities. The outer region of the spray cone is the main contributor to the higher peak; the core region defines the smaller peak. The spectra demonstrate the influence of the air co-flow and atomization air flow: Figure 4a compares the spectra for air co-flows between 20 m³/h and 80 m³/h for a constant atomization air flow of 12.5 slm. An increase of the air co-flow results in an increase of the left peak (low velocities in the outer spray regions). Figure 4b compares the spectra for atomization air flows of 6.5, 12.5 and 18.5 slm at air co-flows of 20 and 80 m³/h. An increase of the atomization air flow shifts the right peak (high velocities in the core region) from 20 m/s to 27 m/s, while the left peak decreases.

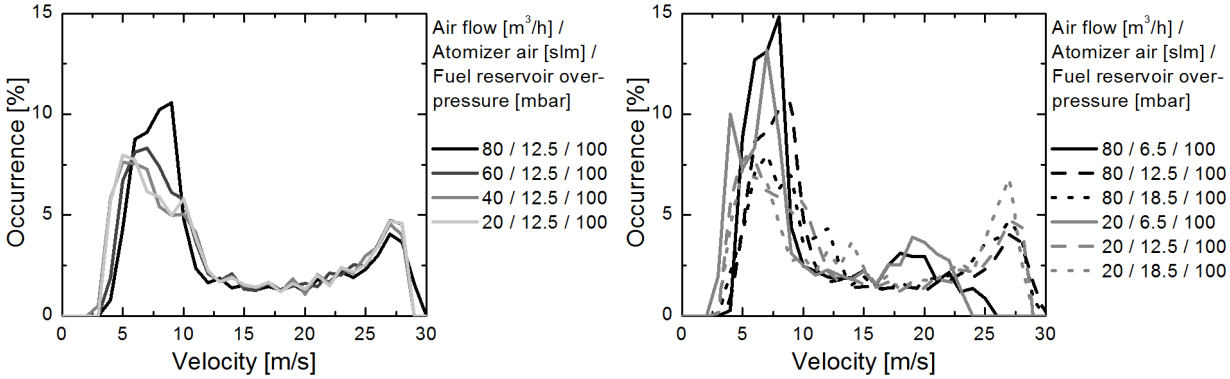

(a) (b)

Figure 4 Velocity spectra: (a) Air co-flow dependency, (b) atomization air flow dependency.

Ignition probability tests

Ignition probability tests on the kerosene spray were carried out to find the most reliable ignition location for a variety of experimental parameters. Tests were performed for air co-flows of 20, 40, 60 and of 80 m³/h, for atomization air flows of 6.5, 12.5 and 18.5 slm and for a reservoir Δp of 100 mbar. Ten trials were performed for each investigated parameter combination. The fuel was Jet A-1 kerosene. Figure 5 shows the results from an overall of 440 ignition tests. Each diagram represents one combination of atomization air flow and reservoir overpressure. Ignition probabilities are given in dependence of the air co-flow and the breakdown distance from the nozzle. An ignition test was only considered successful when it resulted in a stable flame. The error bars are standard deviations, representing the probability uncertainties caused by the limited amount of trials for each measurement series. Figure 6 gives a schematic of the spray cone regions which were tested for their suitability as breakdown locations. The results given in the three diagrams of Figure 5 are interpreted as following:

1) A comparison of Figures 5a to 5c shows, that an increase of the atomization air flow reduces the global ignition probability, regardless of other parameters. An increase of the atomization air flow leads to a narrower spray cone angle. The resulting decrease of the global ignition probability is explained by the fact that the relative location of the breakdown shifts to outer regions of the spray cone (red triangle in Figure 6). The droplet density is very low; the fuel-air ratio is too lean for a flame kernel to develop.

2) The effect of the air co-flow is observable for the 2- to 4-cm-positions: An increase of the air co-flow at a constant atomization air flow reduces the ignition probability (a converse effect for the 1-cm-position is explained at point 4). An increase of the air co-flow leads to a narrower spray cone angle. However, compared to the atomization air flow the effect is much smaller, the influence on ignition probability is small for the 2- and 3-cm-positions.

3) The curves for the 2- to 4-cm-positions show that an increase of the vertical distance decreases the ignition probability. As the radial distance from the centre axis is kept at constant 4 mm, an increase of the vertical distance means that the breakdown location intrudes deeper into the spray cone. This effect is illustrated in Figure 6: at short vertical distances the breakdown is located in the outer regions of the spray cone (red); at longer distances it is located in the inner regions (green). If the breakdown is located deep inside the spray cone (green), several factors may have a negative influence on the ignition probability: First, the energy deposit is reduced, as a significant amount of laser pulse energy is scattered or absorbed by the droplets before reaching the focus. Second, the fuel-air ratio may be too rich for the development of a flame kernel.

4) For a vertical breakdown distance of 1 cm, observations disagree with the mechanisms described under points 1 to 3. In Figures 5b and 5c the black curves illustrate that for low air co-flows the probability decreases with increasing co-flow. This is in agreement with the mechanism described at point 2. But it increases again for very high co-flows. A possible explanation is the recirculation zone directly below the nozzle, which was observed by

PIV measurements in the co-flow (not presented in this paper). The toroidal vortex of the recirculation zone grows with an increase of the air co-flow. At high flow rates the vortex may capture vapor and small droplets, leading to a mixture with high inflammability directly below the nozzle.
In conclusion, the 2-cm-position was the one with the highest overall ignition probability and therefore was chosen as the breakdown location for the PLIF measurements.

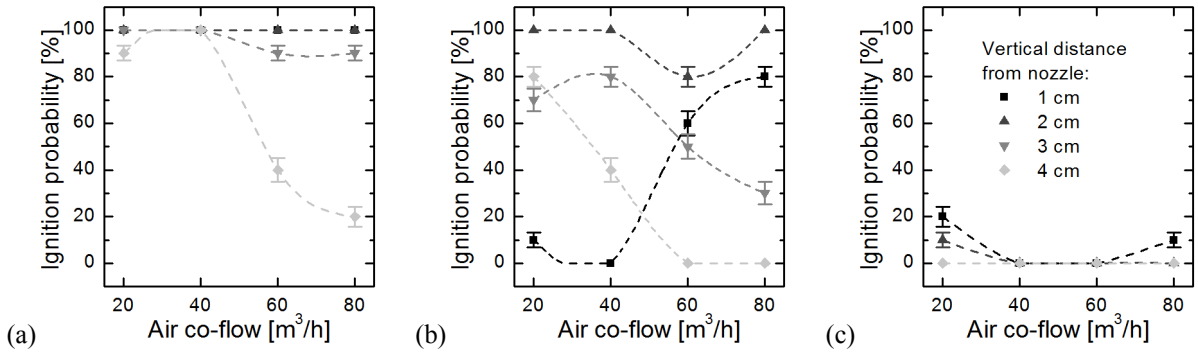

Figure 5 Ignition probabilities: (a) 6.5 slm, (b) 12.5 slm and (c) 18.5 slm atomization air flow.

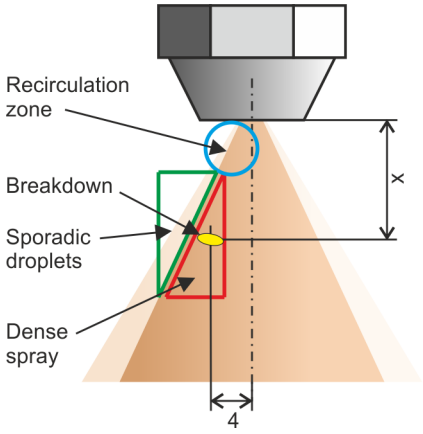

Figure 6 Schematic of the investigated spray cone regions during the ignition probability tests.

Planar Laser-induced Fluorescence measurements

Simultaneous kerosene and OH PLIF measurements were performed to obtain detailed information about the fuel density distribution and flame front location. Measurements were performed for air co-flows of 40 m^3/h and 60 m^3/h and for atomization air flows of 6 and 12 slm and a reservoir Δp of 100 mbar. The fuel was Exxsol D80, which is an aliphatic solvent with kerosene-like physical and chemical properties. The usage of Jet A-1 was not possible because of its very strong fluorescence signal, which results from the high aromatics concentration of about 20 %. The fluorescence signal of Jet A-1 extends from 270 to 420 nm with a maximum between 320 and 340 nm [9] and therefore overlaps with the OH fluorescence. To perform OH PLIF measurements the usage of Exxsol D80 instead of Jet A-1 was necessary, since it only has an aromatics concentration of 0.1 %. However, this is still high enough to see some fuel fluorescence in the images from the OH camera system. Figure 7 shows exemplary instantaneous PLIF images for delays of 1 to 20 ms after the ignition laser pulse. The ignition laser beam entered the field-of-view from the left. The breakdown was located 2 cm below the nozzle and 4 mm off the centre axis. Two images are shown for each delay: the left one shows the fuel PLIF and the right one the OH PLIF. Although the images are 2D cuts through 3D distributions, the axisymmetric nature of the spray allows statements to be made about the flame structure. The distribution of OH radicals reflects the position and shape of the reaction zone and of regions of high temperature. The reaction zones are clearly visible as bright and complex band structures, which quickly spread from the breakdown location to the spray cone edges. The flame stabilizes after only 20 ms, indicating a good mixing of air and vaporized fuel inside the spray. The fuel PLIF images display both the distribution of the liquid and of the vaporized fuel. The liquid fuel appears as a spray pattern at rather weak intensities. In contrast, the fuel vapor shows high intensities and cloudy or filament-like structures. A comparison of the OH and fuel PLIF images provides evidence, that localized fuel-rich zones are sometimes present. These zones are surrounded by OH layers, showing that they feed the nearby chemical reaction zones but are too rich to burn themselves (for example at x = -15 to -20 mm, y = 70 to 90 mm for 20 ms

delay). Average images (not shown) were calculated for every delay to quantify the flame growth and propagation. The transient geometry of the average reaction zones was measured; results are given in Figure 8. The diagrams display the upper and lower flame edge positions, the vertical median position and the area of the OH distribution as a function of time. They provide evidence that the atomization air flow is an important steering parameter for the flame growth and propagation.

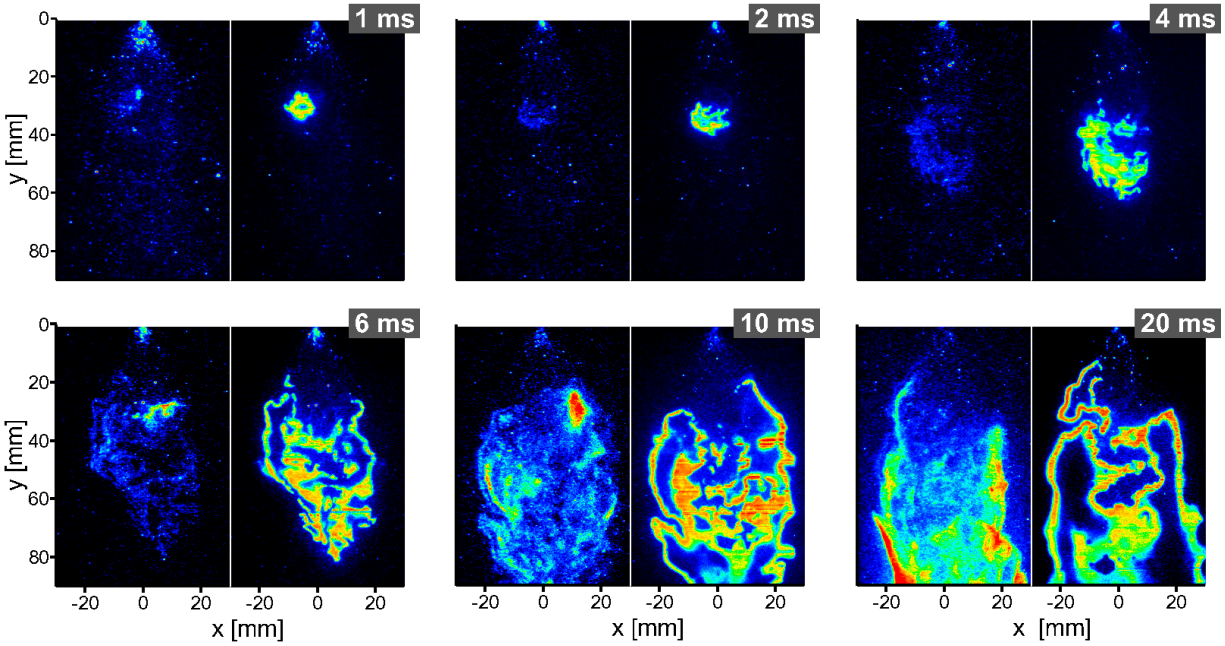

Figure 7 Exemplary PLIF images (6 slm atomization air, 60 m³/h air co-flow). Left: fuel aromatics, right: OH.

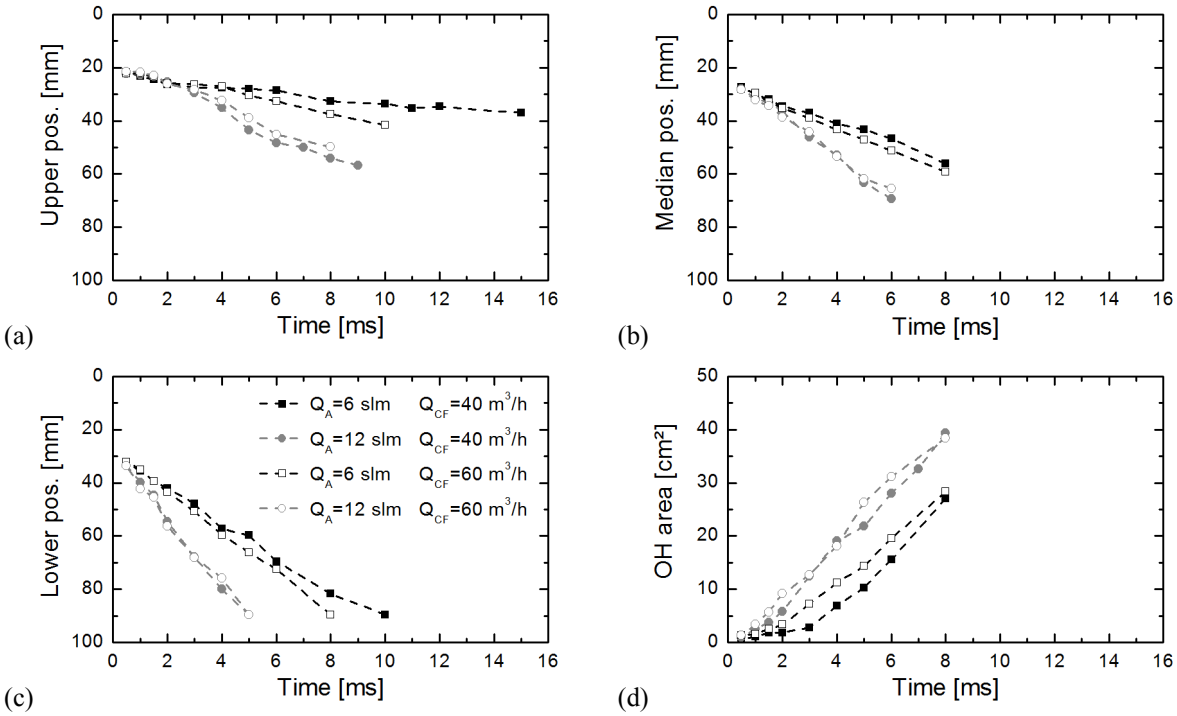

Figure 8 (a) Upper flame edge, (b) vertical median position, (c) lower flame edge, (d) area of OH distribution.

Average flame edge velocities were derived from the diagrams and are given in Table 1. The lower flame edge velocity is significantly higher than the upper one but much slower than the vertical droplet velocities in the core region of the spray, see Figure 3. The diagrams do not explicitly display the phase of flame stabilization, but it was observed that flames stabilize after approximately 20 ms and at upper flame edge positions of 20 to 60 mm below the nozzle, depending on the air co-flow.

Table 1 Average upper and lower flame edge velocities in dependence of the air flows.

Atomization air [slm]	Air co-flow [m^3/h]	Upper flame edge vel. [m/s]	Lower flame edge vel. [m/s]
6	40	1.01 ± 0.07	6.24 ± 0.19
12	40	4.53 ± 0.21	12.85 ± 0.44
6	60	2.07 ± 0.09	7.64 ± 0.10
12	60	4.12 ± 0.23	12.14 ± 0.56

Summary and Conclusions

Experiments regarding the ignition of Jet A-1 spray were performed in a lab-scale model combustor, in order to improve our general understanding of spray ignition processes and to supply validation data for numerical simulations of spray ignition. Ignitions were initiated by laser-induced breakdowns. HS-PIV measurements on spray droplets were performed to measure the droplet velocity distribution and to verify the PIV technique as a tool for spray characterization. The measurements revealed that the spray featured a narrow core region with average droplet velocities extending from 15 to 30 m/s. With rising radius from the centre axis, velocities decreased to approximately 5 m/s and then re-increased to velocities of 8 m/s to 10 m/s near the cone edge. A parameter study revealed the significant impact of the atomization air flow on the spray. An increase leads to narrower cone angles and higher velocities in the core region. An increase of the reservoir overpressure leads to higher droplet velocities in the outer region of the spray cone. The usage of HS-PIV for spray characterization gave satisfying results. The cross correlation algorithm for the vector calculation had to be adjusted very carefully because of the wide range of droplet velocities, which extended from 2 to 30 m/s. However, PIV in sprays generally tends to overestimate the contribution of larger droplets to the average flow field. Zimmer [6] and Husted [7] compared PIV and PDA for spray velocity measurements. Despite the aforementioned restriction of PIV, they found a good agreement between velocities measured with both techniques. Therefore, the data set we obtained with HS-PIV may be subjected to further analyses of the spray dynamics. An ignition probability study was performed to find the most reliable location for the laser-induced breakdown. The vertical distance of the breakdown was shifted and the air flows were varied. The highest global ignition probability was gained when the breakdown was located close to the spray cone edge at the incident side of the laser beam. The local fuel and OH density distributions were simultaneously measured by PLIF. The distribution of the reaction zones, represented by OH structures, is rather complex. A comparison of the OH and fuel PLIF images shows evidence of the presence of fuel-rich zones, where no chemical activities were observed. However, they were typically surrounded by reaction zones. The upper and lower flame edge, the axial median position and the area of the OH density distribution were determined. They indicate that the atomization air flow is an important parameter for the flame growth and propagation. The corresponding average velocities were derived from the slopes. The lower flame edge velocity is higher than the upper flame edge velocity but significantly slower than the average droplet velocity. The presented results are part of an ongoing study. Further experiments are in preparation.

Acknowledgements

This work received funding from the German Federal Ministry of Economics and Technology through the project LuFo IV - GerMaTec (reference number 20T0602).

References

[1] European Aviation Safety Agency, *CS-E 910 / Certification Specifications for Engines*, Amendment 3, December 23, 2010

[2] Lefebvre, A.H., Ballal, D.R., *Gas Turbine Combustion*, Taylor & Francis, 3rd Edition, 2010

[3] Boyde, J., Le Clercq, P., Gebel, G.C., Mosbach, T., Aigner, M., *A Numerical Investigation of the Ignition Characteristics of a Spray Flame under Atmospheric Conditions*, Proceedings of the 50th AIAA Aerospace Science Meeting, AIAA2012-0174, 2012

[4] Boyde, J., Le Clercq, P., Gebel G.C., Mosbach, T., Aigner, M., *Numerical Investigations of the Parameter Govening the Ignitability of a Spray Flame*, Proc. of the ASME Turbo Expo 2012, GT2012-68181

[5] Ikeda, Y., Yamada, N., Nakajima, T., *Multi-intensity-layer Particle Image Velocimetry for Spray Measurement*, Measurement Science and Technology, 11:617-626, 2000

[6] Zimmer, L., *Fuel Droplet Dynamics and Cluster Formation in an Industrial Oil Burner by Planar Droplet Sizing*, Proceedings of the 11th Int. Symp. on Appl. of Laser Techniques to Fluid Mech., 2002

[7] Husted, B., Petersson, P., Lund, I., Holmsted, G., *Comparison of PIV and PDA Droplet Velocity Measurement Techniques on two High-pressure Water Mist Nozzles*, Fire Safety Journal, 44:1030-1045, 2009

[8] Ronney, P.D., *Laser versus Conventional Ignition of Flames*, Optical Engineering, 33:510-521, 1994

[9] Baranger, P., Orain, M., Grisch, F., *Fluorescence Spectroscopy of Kerosene Vapour: Application to Gas Turbines*, Proceedings of the 43rd AIAA Aerospace Science Meeting, AIAA2005-828, 2005